Supplementary Information

Optical Conversion of Conical Intersection to Avoided Crossing

Yasuki Arasaki and Kazuo Takatsuka*
Department of Basic Science, Graduate School of Arts and Sciences,
The University of Tokyo, Komaba, 153-8902, Tokyo, Japan.
E-mail: kaztak@mns2.c.u-tokyo.ac.jp

November 2, 2009

Details of the computation and further discussion of the pulse parameter dependence of the control pulse are given in this supplementary document.

1 Potential Energy Surfaces

The two lowest NO_2 $^2A'$ surfaces, $V_X(\boldsymbol{R})$ and $V_A(\boldsymbol{R})$, used in the present study is the same as that calculated in a previous study [1]. They are obtained as interpolated surfaces over a dense grid of bond lengths and bond angles with the state averaged full valence complete active space self consistent field (CASSCF) method as implemented in the MOLPRO quantum chemistry package [2, 3, 4], using Dunning's correlation consistent polarized triple zeta (cc-pVTZ) basis set [5]. Adiabatic dipole moments in the direction perpendicular to bond angle bisector is also computed together with the potential energy surfaces. The computed surfaces were diabatized with the phenomenological method of Hirsch et al. [6]. Observing that the diabatic

states collectively coincide with the adiabatic states at C_{2v} geometry, and that the dipole moment component perpendicular to the bond angle bisector is zero at C_{2v} geometry and is larger away from that geometry, smallness of this dipole moment component is interpreted to characterize how diabatic the system is. Transformation angle, and hence the relevant transformation matrix, from adiabatic to diabatic representation is obtained through minimizing the diagonal elements of the dipole moment matrix at each geometry. Nonadiabatic coupling elements for the representation obtained this way is confirmed to be small through computation at several representative geometries. The surfaces are thus obtained at rather low cost, but through comparison with other higher level surfaces in the literature [7, 8] we deem adequate for describing the dynamics around the conical intersection.

2 Vibrational Wavepacket Propagation

Vibrational wave functions associated with the two coupled electronic states were represented on a discretized spatial grid in Jacobi coordinates. Molecular orientation is frozen in space because of the ultrashort time span of the conical intersection dynamics. Time dependent Schrödinger equations for the two vibrational wave functions were cast in matrix form and numerically solved with the split operator short time propagator method [9]. Nonadiabatic interaction is handled through diagonalization of the potential energy matrix in the diabatic representation [10]. Kinetic energy terms are handled with the usual FFT grid method [11] for length coordinates and an FFT grid method devised by Dateo and Metiu for the angle coordinate [12]. The adiabatic to diabatic transformation matrix computed to diabatize the potential surfaces were used in reverse to obtain adiabatic observables from the diabatic results. As well as the ground and excited state populations, P_X and P_A, population P^* excited by the pump pulse but excluding the effect of deexcitation by the conical intersection is computed by projecting

out the initial eigenfunction of the electronic ground state left unexcited by the pump pulse from the total vibrational wave function.

3 Control Pulse Parameter Dependence

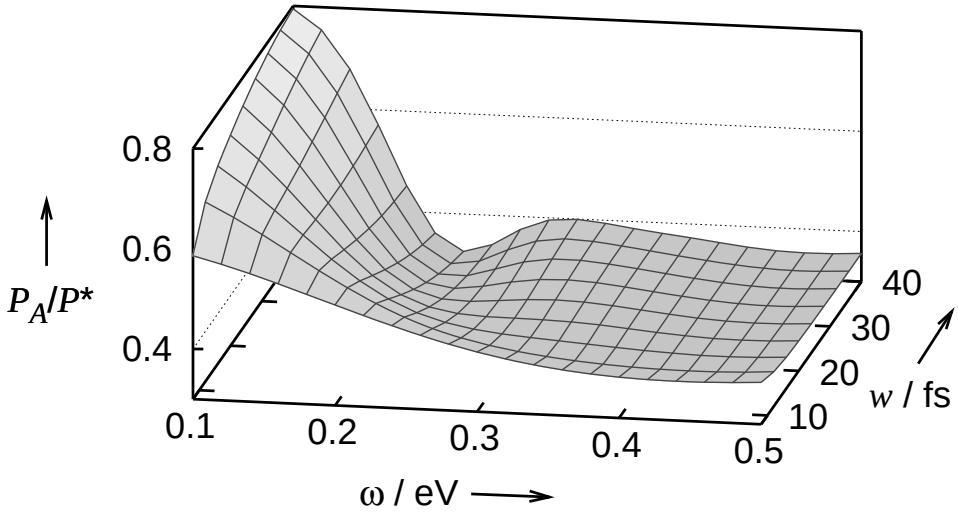

Figure 1: Pulse frequency ω and pulse width w dependence of population ratio left in the excited state P_A/P^* after first passage of the conical intersection region.

The effect of varying the parameters of the control pulse is summarized in Figure 1, in the form of dependence of the ratio of excited state population P_A to population that was initially excited by the pump pulse P^* as a function of control pulse energy ω and pulse width w, at time $t = 16$ fs. Intensity is fixed at $I = 3.2 \times 10^{13}$ W cm^{-2}, center of the pulse $t_0 = 8$ fs, and phase $\phi = 0$ as in the main text.

The time $t = 16$ corresponds to an instant when the system excited by the pump pulse have finished its first passage through the conical intersection region but before the time it returns to the conical intersection region. Increase in the ratio P_A/P^* at this time, compared to $P_A/P^* = 0.3$ for the

case without control pulse, indicate the effectiveness of the control pulse in deforming the conical intersection and suppressing transition through it.

For very low energy pulses $\omega < 0.16$ eV, a wider pulse width enhances the suppression of population transfer through the conical intersection. The period of a single cycle (~ 40 fs) is long enough that during the time wavepacket is passing the conical intersection region, $-\mu_{12}(\boldsymbol{R}_X)E(t)$ remains positive. The field amplitude stays largest for the smallest frequencies. Increase in the pulse width causes the control effect to the conical intersection to begin earlier and last longer.

Near 0.22 eV, however, the trend is reversed. For $\omega = 0.22$ eV, the pulse includes just one half of a cycle during the time the wavepacket cross the conical intersection, and as the pulse width is made larger or frequency higher, the more of the region of field amplitude close to zero enters the time window of wavepacket crossing the conical intersection region. This suppresses the deformation of the conical intersection. As the control pulse energy is made even larger, the field shape begins to include more and more oscillations and the effect the deformation of conical intersection has on the population transfer cancels out. Deformation of the conical intersection causes a significant effect on population transfer only when the period of the control pulse is comparable to the time scale of population transfer.

References

[1] Y. Arasaki and K. Takatsuka, *Chem. Phys.*, 2007, **338**, 175–185.

[2] H.-J. Werner and P. J. Knowles, *J. Chem. Phys.*, 1985, **82**, 5053–5063.

[3] P. J. Knowles and H.-J. Werner, *Chem. Phys. Lett.*, 1985, **115**, 259–267.

[4] H.-J. Werner, P. J. Knowles, R. Lindh, F. R. Manby, M. Schütz, P. Celani, T. Korona, A. Mitrushenkov, G. Rauhut, T. B. Adler, R. D.

Amos, A. Bernhardsson, A. Berning, D. L. Cooper, M. J. O. Deegan, A. J. Dobbyn, F. Eckert, E. Goll, C. Hampel, G. Hetzer, T. Hrenar, G. Knizia, C. Köppl, Y. Liu, A. W. Lloyd, R. A. Mata, A. J. May, S. J. McNicholas, W. Meyer, M. E. Mura, A. Nicklaß, P. Palmieri, K. Pflüger, R. Pitzer, M. Reiher, U. Schumann, H. Stoll, A. J. Stone, R. Tarroni, T. Thorsteinsson, M. Wang and A. Wolf, MOLPRO, version 2006.1, A package of ab initio programs, 2006.

[5] T. H. Dunning, *J. Chem. Phys.*, 1989, **90**, 1007–1023.

[6] G. Hirsch, R. J. Buenker and C. Petrongolo, *Mol. Phys.*, 1990, **70**, 835–848.

[7] V. Kurkal, P. Fleurat-Lessard and R. Schinke, *J. Chem. Phys.*, 2003, **119**, 1489–1501.

[8] S. Mahapatra, H. Köppel, L. S. Cederbaum, P. Stampfußand W. Wenzel, *Chem. Phys.*, 2000, **259**, 211–226.

[9] M. D. Feit, J. A. Fleck and A. Steiger, *J. Comput. Phys.*, 1982, **47**, 412–433.

[10] J. Alvarellos and H. Metiu, *J. Chem. Phys.*, 1988, **88**, 4957–4966.

[11] R. Kosloff, *J. Phys. Chem.*, 1988, **92**, 2087–2100.

[12] C. E. Dateo and H. Metiu, *J. Chem. Phys.*, 1991, **95**, 7392–7400.